Forebrain dopamine neurons project down to a brainstem region controlling locomotion

Dimitri Ryczko[a], Swantje Grätsch[a], François Auclair[a], Catherine Dubé[a], Saskia Bergeron[b], Michael H. Alpert[c], Jackson J. Cone[c], Mitchell F. Roitman[c], Simon Alford[c], and Réjean Dubuc[a,b,1]

[a]Groupe de Recherche sur le Système Nerveux Central, Département de Physiologie, Université de Montréal, Montréal, QC, Canada H3C 3J7; [b]Groupe de Recherche en Activité Physique Adaptée, Département de Kinanthropologie, Université du Québec à Montréal, Montréal, QC, Canada H3C 3P8; and [c]Laboratory of Integrative Neuroscience, University of Illinois at Chicago, Chicago, IL 60607

Edited by Sten Grillner, Karolinska Institutet, Stockholm, Sweden, and approved June 28, 2013 (received for review January 18, 2013)

The contribution of dopamine (DA) to locomotor control is traditionally attributed to ascending dopaminergic projections from the substantia nigra pars compacta and the ventral tegmental area to the basal ganglia, which in turn project down to the mesencephalic locomotor region (MLR), a brainstem region controlling locomotion in vertebrates. However, a dopaminergic innervation of the pedunculopontine nucleus, considered part of the MLR, was recently identified in the monkey. The origin and role of this dopaminergic input are unknown. We addressed these questions in a basal vertebrate, the lamprey. Here we report a functional descending dopaminergic pathway from the posterior tuberculum (PT; homologous to the substantia nigra pars compacta and/or ventral tegmental area of mammals) to the MLR. By using triple labeling, we found that dopaminergic cells from the PT not only project an ascending pathway to the striatum, but send a descending projection to the MLR. In an isolated brain preparation, PT stimulation elicited excitatory synaptic inputs into patch-clamped MLR cells, accompanied by activity in reticulospinal cells. By using voltammetry coupled with electrophysiological recordings, we demonstrate that PT stimulation evoked DA release in the MLR, together with the activation of reticulospinal cells. In a semi-intact preparation, stimulation of the PT elicited reticulospinal activity together with locomotor movements. Microinjections of a D1 antagonist in the MLR decreased the locomotor output elicited by PT stimulation, whereas injection of DA had an opposite effect. It appears that this descending dopaminergic pathway has a modulatory role on MLR cells that are known to receive glutamatergic projections and promotes locomotor output.

motor system | Parkinson disease

Dopamine (DA) neurons of the substantia nigra pars compacta (SNc) and ventral tegmental area (VTA) modulate motor behaviors, including locomotion, through ascending projections to the basal ganglia, the output of which projects to the mesencephalic locomotor region (MLR) (1–3), a brainstem region known to control locomotion in all vertebrate species tested to date (reviewed in ref. 4). DA is known to control the excitability of striatal cells, and a dysfunction of the ascending DA pathway to the striatum is considered to be the main cause for the motor deficits in Parkinson disease (1). However, there have been hints of descending DA projections that would be in position to directly modulate the MLR and hence locomotor activity. In monkeys, DA terminals of unknown origin were observed in the pedunculopontine nucleus (PPN) (5), considered part of the MLR (reviewed in ref. 4). In addition, there is an axonal projection from the SNc to the PPN in rats, but the transmitter system is unknown (6).

We examined the DA system in a basal vertebrate, the lamprey, and found a previously unknown descending DA pathway from the posterior tuberculum (PT) to the MLR, which comprises the PPN and the laterodorsal tegmental nucleus (LDT) in lampreys (ref. 7; reviewed in ref. 4). In lampreys, the PT is considered homologous to the SNc and/or VTA of mammals because of its DA projection to the striatum (3). Further, we determined a role for this DA pathway in the control of locomotion.

Results

Descending DA Projections from the PT to the MLR. Immunofluorescence against tyrosine hydroxylase (TH) or against DA was used to visualize PT neurons containing DA. The distribution of TH and DA immunoreactive cell bodies and fibers were very similar in the PT and the MLR (Fig. S1 *A–F*). Fibers and varicosities positive for TH (n = 8 animals) or DA (n = 3 animals) were present throughout the LDT and the PPN (Fig. 1 *B* and *C* and Fig. S1 *A–C*), both considered parts of the MLR (ref. 7; reviewed in ref. 4). TH-positive terminals were found in close proximity to cholinergic MLR cell bodies and dendrites (Fig. 1 *A–D*) and in the vicinity of MLR cells traced from the middle rhombencephalic reticular nucleus (MRRN; n = 5 animals; Fig. 1 *E–G*). The location of tracer injection sites in the MRRN was verified by histologic examination (Fig. S2 *A* and *B*). As the MLR cholinergic projection to the reticular formation can initiate locomotion (7, 8), the juxtaposition of TH-positive terminals suggests that they are in position to directly modulate locomotor output.

We looked for the origin of this DA projection by using tracer injections in the MLR coupled with TH immunofluorescence. The MLR was considered to overlap largely with the cholinergic neuronal population of the isthmic region, with the conspicuous Müller cell I1 lying at the caudal limit as a landmark (detailed description provided in ref. 9). The PT refers to a region of the caudal diencephalon located ventral to the pretectum. The PT contains a prominent population of dopaminergic neurons, some of them projecting to the striatum, that are intensely labeled by

Significance

We found in lampreys that dopaminergic cells from the posterior tuberculum (homologue of the mammalian substantia nigra pars compacta and/or ventral tegmental area) not only send ascending projections to the striatum, but also have a direct descending projection to a brainstem region controlling locomotion—the mesencephalic locomotor region—where it releases dopamine (DA). DA increased locomotor output through a D1 receptor-dependent mechanism. The presence of this descending dopaminergic projection may have considerable implication for our understanding of the role of DA in motor control under physiological and pathological (i.e. Parkinson disease) conditions.

Author contributions: D.R., F.A., and R.D. designed research; D.R., S.G., F.A., C.D., S.B., M.H.A., J.J.C., M.F.R., S.A., and R.D. performed research; D.R., S.G., F.A., C.D., S.B., M.H.A., J.J.C., M.F.R., S.A., and R.D. analyzed data; and D.R., F.A., and R.D. wrote the paper.

The authors declare no conflict of interest.

This article is a PNAS Direct Submission.

[1]To whom correspondence should be addressed. E-mail: rejean.dubuc@gmail.com.

This article contains supporting information online at www.pnas.org/lookup/suppl/doi:10.1073/pnas.1301125110/-/DCSupplemental.

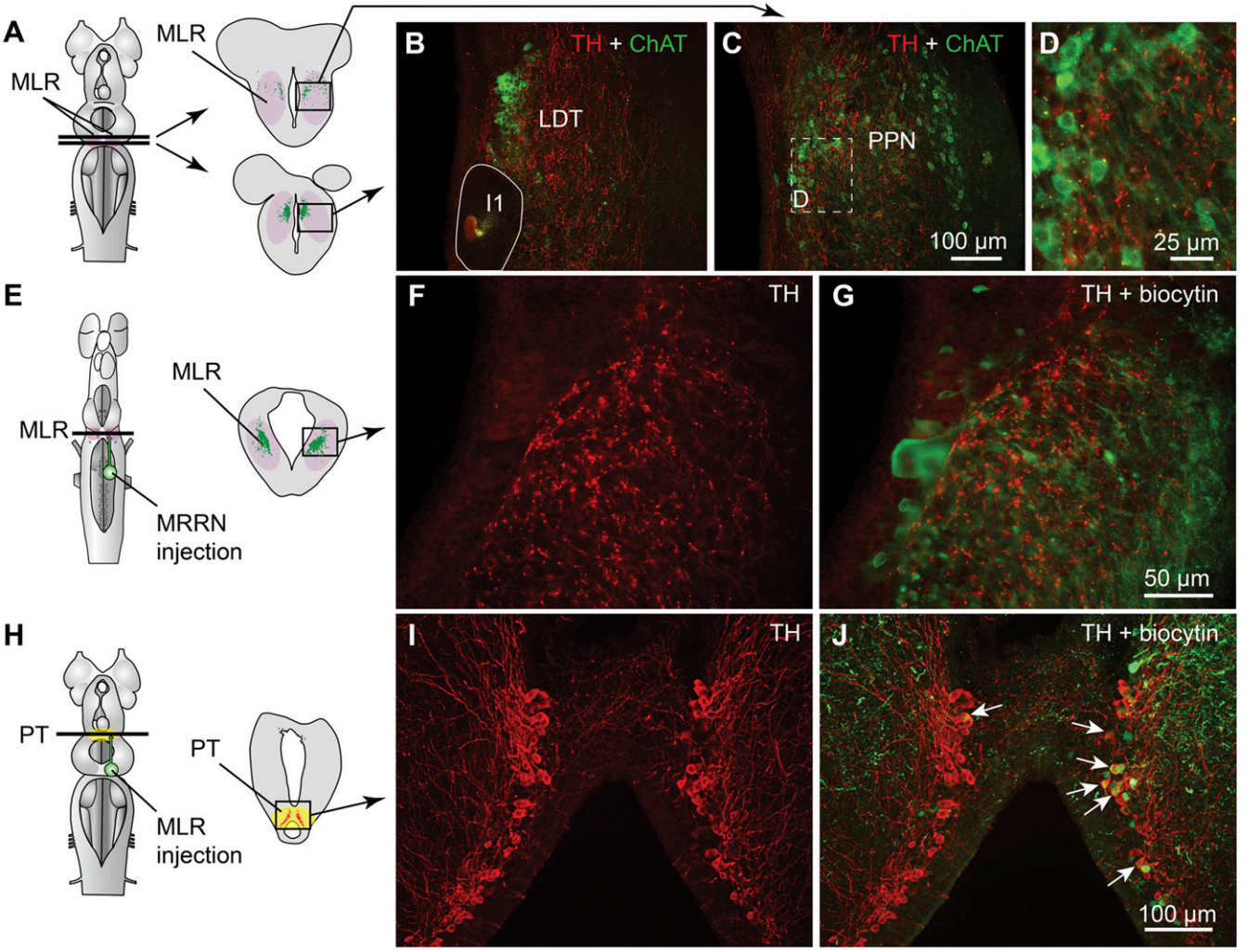

Fig. 1. Dopaminergic (DA) neurons of the PT send descending projections to the MLR. (*A–D*) TH (red)-containing fibers and varicosities in proximity with MLR cells positive for ChAT (green) in the LDT and the PPN in adult lampreys. The giant I1 reticulospinal cell is outlined in *B*. (*D*) Magnification of the dashed rectangle in *C*. (*E–G*) Fibers and varicosities immunoreactive to TH (red) surrounded the laterally oriented dendrites of MLR cells retrogradely labeled from an injection of the tracer biocytin (green) in the reticulospinal population of the MRRN in larval lampreys. (*H–J*) A unilateral injection of the tracer biocytin in the MLR (*H*, *Right*, green) followed by immunofluorescence against TH (*I*, red) revealed double-labeled cells in the PT (white arrows, *J*). The innervation of the MLR by TH-positive fibers was very similar in larval and adult lampreys.

TH immunofluorescence (3). The rostrocaudal extent of the population in spawning phase animals is around 500 μm, spreading approximately 100 to 300 μm from the midline (Fig. 1 *H–J*). The PT contained 189 ± 21 TH-positive cells (n = 12 animals). Many TH-positive cells of the PT were retrogradely labeled from MLR tracer injections (24 ± 3 cells, i.e., 15.4 ± 2.4%), largely on the ipsilateral side (2 ± 1 cells labeled contralaterally, i.e., 1.6 ± 0.6%; n = 6 animals; Fig. 1 *H–J*). Again, these results were confirmed by DA immunofluorescence (n = 3 preparations; Fig. S1 *G–I*). It is noteworthy that retrogradely labeled neurons were found only among the intensely labeled TH-positive population of the PT (outlined in Fig. S1 *E* and *F*), both in the dorsomedial portion that contains larger neurons and in the lateroventral portion that contains smaller neurons. No labeled cells were found in the periventricular TH (and DA) neuron population of the mammillary area, or in any other TH-positive cell population of the brain and spinal cord. By using triple labeling, we found that DA cells in the PT projecting to the striatum were intermingled with those projecting to the MLR (n = 4 preparations; Fig. 2). In all cases, occasional TH-positive neurons of the PT (n = 1–2 cells) were found to project to the MLR and the striatum (Fig. 2*E*). Overall in the PT, TH-positive neurons with descending projections to the MLR (n = 16–52 cells) were, on average, 11 ± 2 times more numerous than those with ascending projections to the striatum (n = 1–5 cells; n = 4 animals).

Activation of the Locomotor System by Stimulation of the PT. Physiological experiments were carried out to examine the role of this descending DA projection in motor control. For this purpose, a semi-intact preparation was used in which the activity of reticulospinal cells is recorded intracellularly while the body freely swims in the chamber. Trains of stimuli applied to the PT (10-s train, 4–5 Hz, 4–30 μA, 2-ms pulses) elicited reticulospinal cell discharges and swimming (n = 13 preparations; Fig. 3 *A–E*). The location of the stimulation sites was confirmed by histologic examination (Fig. 3*D*). Chemical stimulation of the PT with local microinjections of 3.0 to 8.0 pmol of D-glutamate (5 mM, 17–43 pulses of 20 ms, 0.6–1.6 nL per microinjection) into the site used for electrical stimulation, was confirmed to elicit locomotion and reticulospinal discharges in one preparation. This is consistent with previous observations that electrical or chemical stimulation

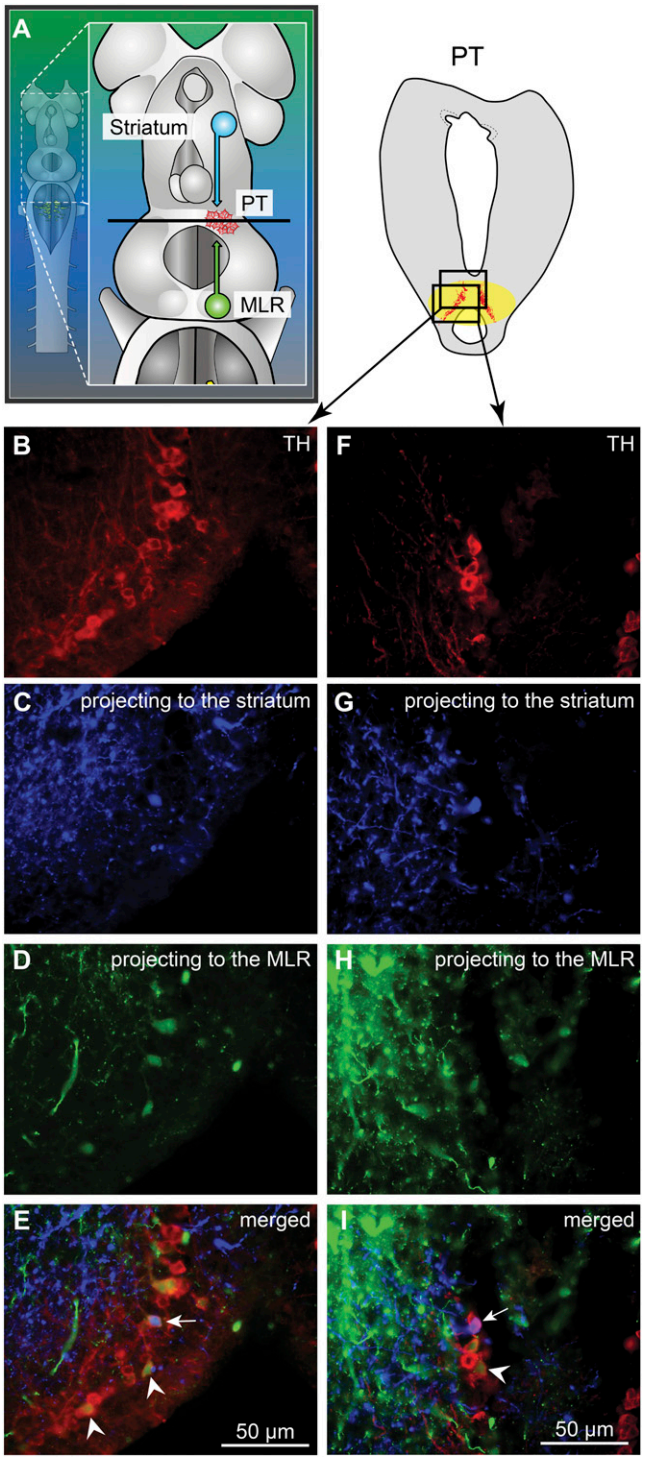

Fig. 2. TH-positive cells projecting to the striatum or to the MLR are intermingled in the PT as shown in triple-labeling experiments. (*A*) Dorsal view of a lamprey brain showing the injection sites of the tracers in the MLR (green) and in the striatum (blue). (*B–E* and *F–I*) Photomicrographs of two examples of transverse sections in the PT at the level indicated on the diagram in *A*. (*Top Right*) Diagram illustrates a cross-section at the level of the PT with the approximate location of the photomicrographic frames shown in *B–I*. DA cells of the PT were labeled with immunofluorescence against TH (red, *A, B,* and *F*). Some cells of the PT were retrogradely labeled by a unilateral injection of one tracer in the striatum (blue, *A, C,* and *G*). Some cells of the PT were retrogradely labeled by another tracer injection, this time in the MLR (green, *A, D,* and *H*). (*E*) The photomicrographs from *B–D* were merged to show the three markers. White arrowheads indicate some examples of TH-positive cells of the PT that project to the MLR, whereas the white arrow points to a TH-positive cell projecting to the MLR and the striatum. (*I*) The photomicrographs from *F–H* were merged. The white arrowhead indicates a PT cell projecting to the MLR and containing TH. The white arrow points to a cell that projects to the striatum and contains TH.

with D-glutamate of this region initiates locomotion (10, 11). By using targeted whole-cell patch clamp recordings in an isolated brain preparation (*Materials and Methods*), we found that trains of stimuli (10-s train, 4–5 Hz, 10–35 μA, 2-ms pulses) to the PT (Fig. S2 *G* and *H*) directly activate MLR cells projecting to reticulospinal neurons ($n = 6$ cells from six preparations; Fig. 3 *F–I*). When comparing simultaneous recordings from an MLR cell and reticulospinal cells (extracellular), we found a very similar activation following trains of stimuli to the PT (Fig. 3*H*). Single stimuli to the PT evoked short-latency, large excitatory postsynaptic currents in whole-cell patch recorded MLR cells (Fig. 3*I*). Glutamatergic receptors are involved in these responses, as previously demonstrated (10), and the DA input from PT to the MLR could modulate this glutamatergic excitatory connection. The rest of our study was aimed at examining this possibility.

Stimulation of the PT Evokes DA Release in the MLR. Fast-scanning cyclic voltammetry (12) was used to measure changes in DA concentration in the MLR while stimulating the PT (Fig. 4). The location of the recording site was confirmed to be within the MLR (Fig. S2 *J* and *K*). A reticulospinal neuron was recorded intracellularly to monitor locomotor network activation. Trains of stimuli (10-s train, 5 Hz, 14–25 μA, 2-ms pulses) in the PT (Fig. S2 *G* and *I*) elicited a large increase in DA concentration in the MLR ($n = 6$ preparations; Fig. 4 *A–C*). We found a strong positive correlation between the increase in DA concentration in the MLR elicited by PT stimulation and the increase in the number of spikes per unit time in reticulospinal cells recorded during the same trials ($R = 0.91$; $P < 0.001$; $n = 30$ stimulations in six preparations; Fig. 4 *D* and *E*). DA release in the MLR was also evoked together with reticulospinal spiking activity when chemically activating the PT with local microinjections of 60.5 pmol of D-glutamate (5 mM, 10 pulses of 100 ms, 12.1 nL per microinjection; $n = 20$ stimulations in four preparations; Fig. S3). These data demonstrate that PT activation results in DA release in the MLR and suggest that DA release may contribute to locomotor output.

Blockade of the DA Inputs to the MLR Decreases Locomotor Output. We then tested whether DA had an effect on the locomotor output elicited by PT stimulation (10-s train, 5 Hz, 12–30 μA, 2-ms pulses). Bath-applying DA (10 μM) onto the brain induced a 25% decrease in the PT stimulation intensity threshold required to elicit locomotion in two of three semi-intact preparations [reduction from 16 to 12 μA in both cases (Fig. S4 *A–C*); 20 μA in the remaining preparation in which no effect was observed]. For PT stimulation intensities above locomotor threshold (16–30 μA), bath-applied DA increased locomotor bout duration (+86.8 ± 18.4%; $P < 0.001$ vs. control), the number of locomotor cycles (+102.6 ± 23.8%; $P < 0.001$), and locomotor frequency (+25.8 ± 9.1%; $P < 0.01$; pooled data from three preparations, 18 bouts, and six intensities per preparation; Fig. S4 *D–F*). These effects were reduced after DA washout ($P < 0.05$ or $P < 0.001$ vs. DA). Bath-applied DA also increased the number of reticulospinal spikes (+72.4 ± 17.9%; $P < 0.001$ vs. control) and the duration of spiking activity (+58.4 ± 14.7%; $P < 0.001$ vs. control). These increases were also reversed after approximately 1 h of DA washout ($P < 0.01$ vs. DA in both cases).

Next, we determined that DA has a direct excitatory effect on the MLR. Microinjections of 1.0 to 7.0 pmol of DA (5 mM, $n =$ 5–38 pulses of 20 ms, 0.2–1.4 nL per microinjection) in the MLR

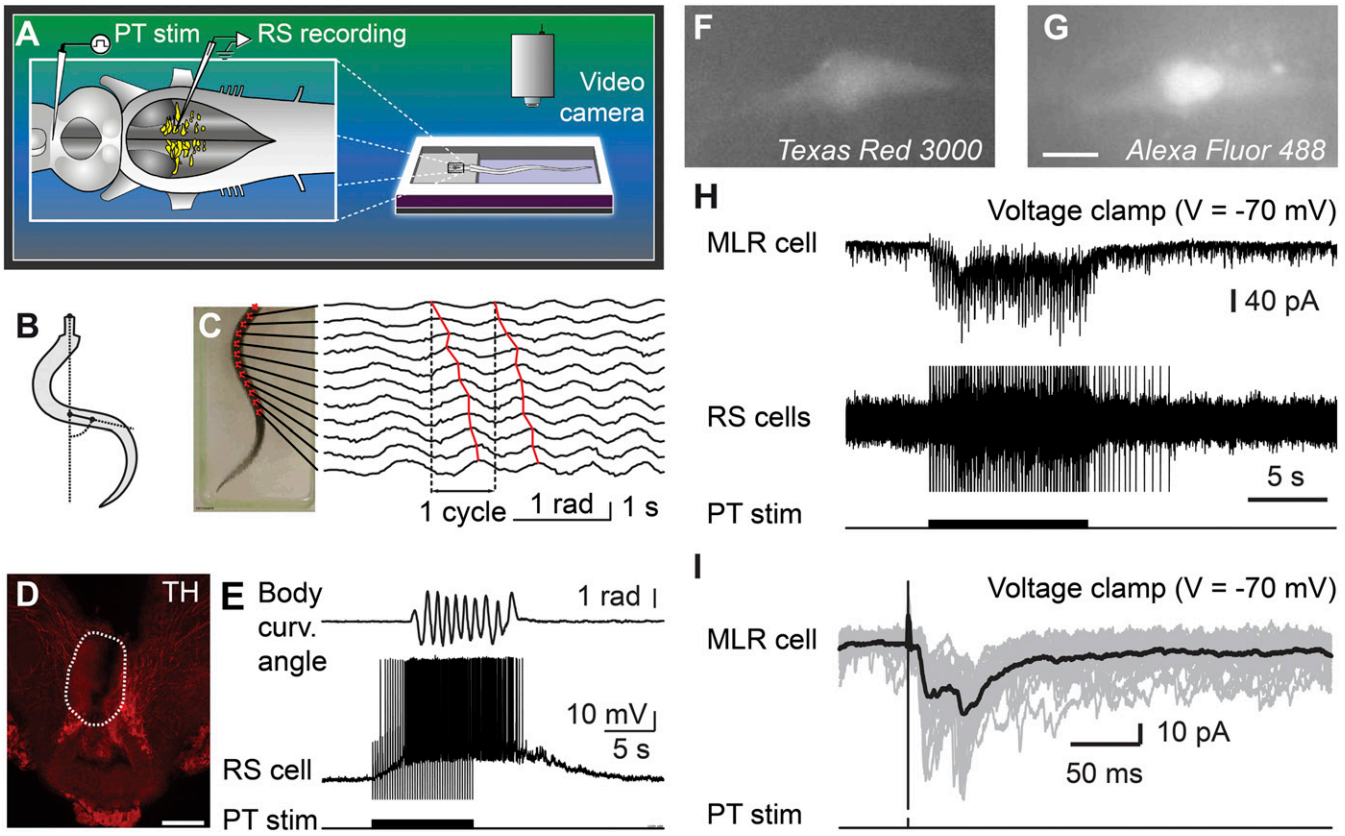

Fig. 3. Stimulation of the PT activates brainstem locomotor circuits. (*A–E*) In a semi-intact preparation, the PT was stimulated and the reticulospinal (RS) cells were recorded together with locomotor movements. (*B* and *C*) Body curvature oscillations during locomotion. (*C*) PT stimulation (10-s train, 5 Hz, 11 μA, 2-ms pulses) elicited swimming as illustrated by the rostrocaudal mechanical wave. (*D*) The PT stimulation site was confirmed histologically by an electrolytic lesion (enclosed by white dashed line) that colocalized with TH-immunoreactive neurons (red). (Scale bar: 200 μm.) (*E*) PT stimulation elicited reticulospinal activity together with swimming. Stimulation artifacts were clipped. (*F–I*) Whole-cell patch-clamp recordings of MLR neurons retrogradely labeled from an injection of dextran amines conjugated to Texas red (MW, 3,000 Da) in the MRRN. (*F* and *G*) MLR neuron labeled by the Texas red–dextran amine injection in the MRRN and by the fluorescent marker added to the patch pipette solution (Alexa Fluor 488 hydrazide). (Scale bar: 10 μm.) (*H*) Trains of stimuli (10-s train, 5 Hz, 7 μA, 2-ms pulses) activated the whole-cell patch-clamped MLR neuron concomitantly with reticulospinal neurons, which were used to monitor locomotor activation. Action potentials were recorded extracellularly from reticulospinal neurons of the MRRN, and stimulation artifacts were clipped. (*I*) Single pulse PT stimulation (0.1 Hz, 7 μA, 2-ms pulses) elicited short-latency excitatory postsynaptic currents in MLR neurons. (*H* and *I*) Data from two different animals.

(as confirmed by histologic examination; Fig. S2 *J* and *L*) increased the locomotor output elicited by trains of electrical stimulation (10-s train, 5 Hz, 4–7 μA, 2-ms pulses) in the PT (Fig. 3*D*) in a semi-intact preparation ($n = 25$ injections in five preparations; Fig. 5 *A–C*). DA microinjections prolonged the locomotor bout duration (+56.7 ± 14.3%; $P < 0.001$) and increased the number of locomotor cycles (+50.8 ± 12.3%; $P < 0.001$). These effects were reversed after DA washout ($P < 0.05$ vs. injection in both cases; Fig. 5*C*). DA injections in the MLR also increased the duration of reticulospinal cell spiking activity (+33.6 ± 11.8%; $P < 0.01$). This effect was reversed after approximately 1 h of washout ($P < 0.01$; Fig. 5*C*). The effects on locomotor threshold were not measured in these experiments. The excitatory effect of DA microinjections in the MLR was lower than that of bath-applied DA, probably because of the single site of action of DA during local microinjections. For instance, local DA microinjections in the MLR did not significantly modify the locomotor frequency that remained at 95.2 ± 3.0% of control ($P > 0.05$), or the number of reticulospinal spikes that remained at 119.5 ± 11.1% of control ($P > 0.05$).

D1 receptor activation is known to have excitatory effects on striatal cells in mammals (reviewed in ref. 13). Those receptors are also present in lampreys (14, 15). Targeted blocking of D1 receptors in the MLR (Fig. S2 *J* and *L*) dramatically decreased the locomotor output elicited by stimulation of the PT (10-s train, 5 Hz, 7–11 μA, 2-ms pulses; Fig. 3*D*). Local microinjection of 0.1 to 0.8 pmol of the D1 antagonist SCH 23390 (500 μM, 6–43 pulses of 20 ms, 0.2–1.6 nL per microinjection) in the MLR ($n = 25$ injections in five preparations; Fig. 5 *D–F*) decreased the duration of locomotor bouts (−48.4 ± 10.6%; $P < 0.001$ vs. control), locomotor frequency (−32.2 ± 6.3%; $P < 0.001$), and the number of locomotor cycles (−60.0 ± 9.9%; $P < 0.001$). These decreases in locomotor output were reversed after washout (for all parameters, $P < 0.001$ vs. injection; Fig. 5*F*). Blocking D1 receptors in the MLR also decreased the duration of spiking activity in reticulospinal neurons (−43.8 ± 9.4%; $P < 0.001$ vs. control), their discharge frequency (−30.8 ± 9.9%; $P < 0.01$), and their number of spikes (−41.6 ± 11.9%; $P < 0.001$). Recovery was obtained after approximately 1 h of washout ($P < 0.05$ or $P < 0.01$ vs. injection; Fig. 5*F*).

Discussion

Newly Identified Descending DA Pathway. In this study, we provide evidence for a descending DA projection from the PT to the MLR that modulates motor output. This descending DA pathway supports DA release, which increases locomotor output, and D1 receptors are involved in this excitatory effect. It appears that this descending DA pathway amplifies the previously known excitatory glutamatergic inputs to MLR cells (10). Such a descending DA projection is also very likely to be present in

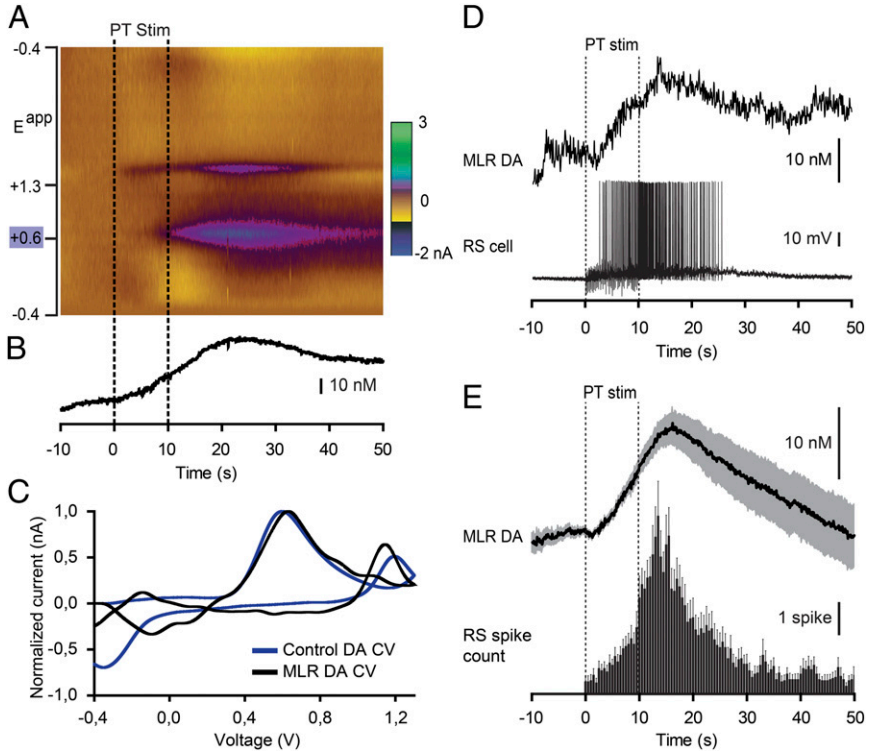

Fig. 4. Stimulation of the PT evokes DA release in the MLR together with reticulospinal (RS) activity. (*A*) DA release evoked by PT stimulation (PT Stim, 10-s train, 5 Hz, 15 μA, 2-ms pulses) in an isolated brain preparation (stimulation period = 0–10 s). The color plot depicts current changes (in color) across the applied voltages (E^{app}; i.e., ordinate) over time (i.e., abscissa). DA is identified by its oxidation peak (~0.6 V) that appears during PT stimulation. (*B*) Changes in DA concentration in the MLR extracted from *A*. (*C*) Plots of normalized current vs. voltage. The DA electrochemical signal (cyclic voltammogram; CV) recorded from the MLR in *A* (black) is similar ($R = 0.82$, $P < 0.001$) to that measured from a 1-μM control DA solution (blue) bath-applied following the experiment, thus confirming DA detection. (*D*) The DA release in the MLR elicited by PT stimulation was positively correlated with the number of spikes evoked in reticulospinal cells. (*E*) Changes in DA concentration plotted vs. the number of reticulospinal spikes per unit time (bin represents 500 ms) in the same trials ($n = 30$ stimulations from six preparations). Mean ± SEM are illustrated.

mammals, although not yet described. For instance, there is a projection from the SNc to the PPN in rats (6), and DA terminals are present in the PPN in monkeys (5). We now confirm in lampreys that DA neurons in the PT project to the striatum as previously described (3). This supports the idea that the lamprey PT is homologous to the SNc and/or VTA of other vertebrates, including other fishes (16, 17), amphibians (18), birds and mammals (reviewed in ref. 19), and humans (20). Moreover, a recent series of studies demonstrated in detail that the basic organization of the basal ganglia, which are target structures of the PT, have physiological and anatomical features that are very similar to those of birds and mammals (refs. 2, 15, 21–25; reviewed in ref. 26). These interesting studies demonstrated that forebrain structures are highly conserved in vertebrates. Therefore, ascending and descending projections of DA cells of the SNc and/or VTA are very likely to have been conserved in vertebrates.

Functional Significance. The presence of a direct DA pathway from SNc/VTA to the MLR may have significant implications for our understanding of the role of DA in motor control under normal and pathological conditions. For instance, DA inputs to the MLR could be involved in the increased exploratory behavior elicited by a novel stimulus, to which a large part of DA neurons are known to respond (reviewed in ref. 27). This pathway could also play a role in the well-documented locomotor effects of the DA drugs of abuse (e.g., hyperlocomotor effects of psychostimulants). In patients with Parkinson disease, DA neurons from the SNc/VTA undergo degeneration, which affects their ascending inputs to the basal ganglia. The descending DA projection we now describe should also be affected and play a role in the locomotor deficits. Interestingly, a depletion of DA terminals was recently shown in the PPN of monkeys treated with 1-methyl-4-phenyl-1,2,3,6-tetrahydropyridine (MPTP) (5), a molecule that has been used extensively in mammals to mimic the motor deficits observed in Parkinson disease. Interestingly, forebrain DA depletion in lampreys injected with MPTP is also associated with severe locomotor deficits, characterized by a decrease in the initiation and maintenance of locomotor activity (28). The locomotor deficits in these pathological conditions may involve, at least in part, the loss of the excitatory DA input to the MLR we describe here. Taken together, these observations suggest that the descending DA projection we report here is conserved across vertebrates and is compromised by the death of DA cells in the SNc/VTA. As such, our results thus provide insights into the role of DA cells of the SNc/VTA in locomotor control.

Materials and Methods

All procedures conformed to the guidelines of the Canadian Council on Animal Care and Association for Assessment and Accreditation of Laboratory Animal Care, and were approved by the animal care and use committee of the Université de Montréal, the Université du Québec à Montréal, and the University of Illinois at Chicago. Care was taken to minimize the number of animals used and their suffering.

Animals. Experiments were performed on 33 larval, 5 newly transformed, and 17 spawning-phase sea lampreys (*Petromyzon marinus*). Larval and newly transformed animals were collected in the wild from the Morpion stream (Québec, Canada) or the Pike River (Québec, Canada), or purchased from ACME Lamprey. Spawning-phase lampreys were captured during their spring run in the Great Chazy river (New York) and given to us by the US Fish and Wildlife Service of Vermont. The animals were kept in aerated water at 5 °C.

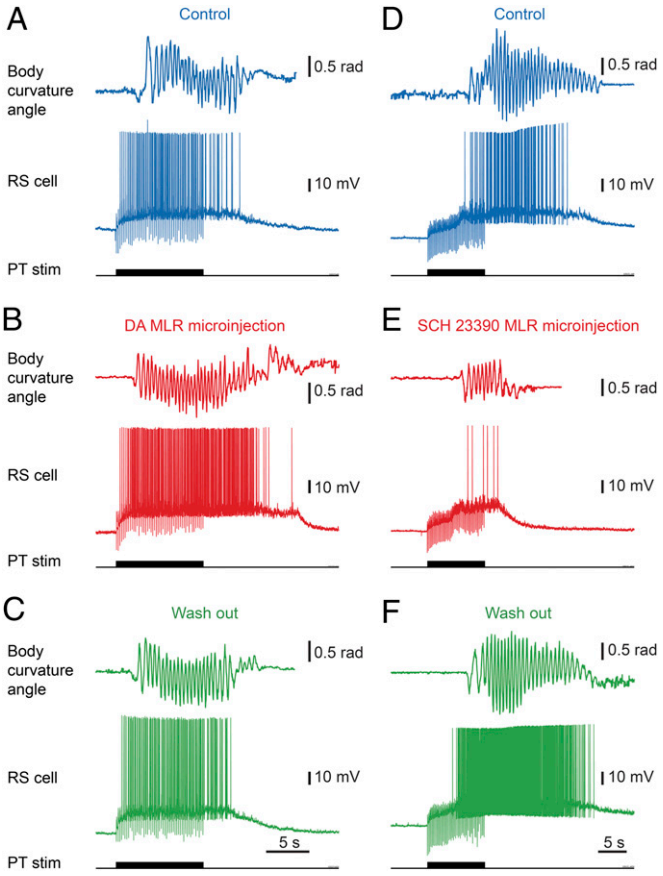

Fig. 5. The descending dopaminergic (DA) projection from the PT to the MLR controls locomotion. DA or the D1 antagonist SCH 23390 was microinjected in the MLR with a Picospritzer in a semi-intact preparation. (*A*–*C*) Microinjection of DA (5 mM; *Materials and Methods*) in the MLR increased the locomotor and reticulospinal (RS) activities elicited by PT stimulation (10-s train, 5 Hz, 6 μA, 2-ms pulses). (*D*–*F*) Microinjection of the D1 antagonist SCH 23390 (500 μM; *Materials and Methods*) in the MLR decreased the locomotor output elicited by PT stimulation (10-s train, 5 Hz, 11 μA, 2-ms pulses). In both cases, the locomotor response and the corresponding reticulospinal activity are illustrated. Blue indicates control condition, red indicates microinjection of DA compounds in the MLR, and green indicates washout.

Surgical Procedures. The animals were anesthetized with tricaine methanesulfonate (MS 222; 100 mg/L) and then transferred in a cold oxygenated Ringer solution (8–10 °C, 100% O_2) of the following composition (in millimolar): 130 NaCl, 2.1 KCl, 2.6 $CaCl_2$, 1.8 $MgCl_2$, 4 Hepes, 4 dextrose, and 1 $NaHCO_3$ (pH 7.4). For anatomical experiments, the whole brain was then isolated in vitro and injected with anatomical tracers as described later. A total of 5 larval and 17 spawning-phase animals were used for the anatomical experiments.

Anatomical Tracing. Biocytin was used for retrograde tracing experiments. In the case of double labeling, biocytin and Texas red–dextran amines were used. For both tracers, the injection site was first lesioned with a pulled glass micropipette. Crystals of the tracers were immediately placed inside the lesioned site to dissolve for 10 min, and then the whole brain was rinsed thoroughly for 5 min, including the injection site. The tracer injection sites were chosen on the basis of previous anatomical and physiological studies [MRRN and MLR (refs. 7–10; reviewed in ref. 4) and striatum (2, 3, 23)] and verified by histologic examination (Fig. S2). The preparations were then transferred into a dark refrigerated chamber and continuously perfused with new, oxygenated Ringer solution overnight for retrograde transport of the tracer to occur. The following day, the preparations were transferred into a fixative solution chosen according to the immunofluorescence procedure to follow (as detailed later).

Immunofluorescence. Experimental procedures for immunofluorescence against TH, choline acetyltransferase (ChAT), or DA were undertaken immediately after anatomical tracing. Fixation of the tissue was the first step. For TH and ChAT, the neural tissue was immersed in 4% (wt/vol) paraformaldehyde in PBS solution (0.1 M, pH 7.4, 0.9% NaCl) for 24 h and then transferred to a phosphate-buffered 20% (wt/vol) sucrose solution. For DA, the neural tissue was first immersed for 5 min in 0.1 M cacodylate buffer, pH 6.2, containing 0.9% sodium metabisulfite (MBS), followed by 55 min in 0.1 M cacodylate buffer, pH 7.5, containing 0.9% MBS. The tissue was then rinsed thoroughly with 0.05 M Tris buffer containing 0.9% MBS (TBMBS) and transferred overnight to another vial containing the same solution with 20% (wt/vol) sucrose. The brain tissue was sectioned transversely at 25-μm thickness with a cryostat, and the sections were collected on ColorFrost Plus microscope slides (Fisher Scientific) and air-dried overnight on a warming plate. If biocytin had been injected as a tracer, the sections were first rinsed three times, 10 min each, before being incubated for 30 min in PBS solution (or TBMBS for DA) containing a 1:200 dilution of streptavidin–Alexa Fluor 594, 488, or 350 (Invitrogen), depending on the color needs. The sections were then rinsed again three times for 10 min each with PBS solution (or TBMBS).

For ChAT immunofluorescence, the sections were then preincubated in a PBS solution containing 0.3% Triton X-100 and 5% (vol/vol) normal horse serum for 60 min. The sections were then incubated in the same preincubation solution containing a goat anti-ChAT antibody (diluted 1:80; AB144P; Millipore) overnight at 4 °C. The following day, the sections were rinsed three times for 10 min each in PBS solution and incubated in the preincubation solution containing a donkey anti-goat Alexa Fluor 488 antibody (diluted 1:200; A11055; Invitrogen) for 60 min. The sections were then rinsed three times for 10 min each with PBS solution and once with deionized water, and left to dry on a warming plate for 5 min. The slides were then mounted with Vectashield with or without DAPI (H1000 or H1200; Vector).

For TH immunofluorescence, normal goat serum was used instead of normal horse serum, and the antibodies used were a rabbit anti-TH (diluted 1:400; AB152; Millipore) and a donkey anti-rabbit Alexa Fluor 594 (diluted 1:400; A21207; Invitrogen) or a goat anti-rabbit Alexa Fluor 488 (1:400; A11008; Invitrogen). All other steps were as described for ChAT immunofluorescence. TH immunofluorescence was used to visualize DA neurons. This choice was based on other studies in lampreys (3, 29, 30).

For DA immunofluorescence, PBS solution was replaced with TBMBS, Triton X-100 was increased to 0.5%, and 5% (vol/vol) normal goat serum was used as for TH. The antibodies used were a mouse anti-DA (diluted 1:400; MAB5300; Millipore) and a goat anti-mouse DyLight 594 (diluted 1:200; 115-515-146; Jackson ImmunoResearch). All other steps were as described for ChAT immunofluorescence.

Specificity of the fluorescent secondary antibodies was verified by omitting the primary antibody from the procedures described earlier. In every case, no labeling was obtained under these conditions. The AB144P antibody has been used on lampreys for many years by different research teams, and its selectivity against ChAT is well demonstrated (7, 31, 32). The AB152 antibody against TH has been used reliably on lampreys in many independent studies on DA neurons (24, 33, 34). The specificity of the MAB5300 antibody for DA was tested by ELISA by the manufacturer, and its pattern of labeling in our material corresponded closely to that reported with other DA antibodies in the lamprey (29, 30).

The sections were then observed and photographed using an E600 epifluorescence microscope equipped with a DXM1200 digital camera (Nikon). Combining digital photomicrographs taken with different filter sets and adjusting the levels so that all fluorophores were clearly visible simultaneously was done by using Photoshop CS5 (Adobe). To avoid double counting as a result of the sectioning of the tissue, cells were counted on only half the sections, skipping one in between. The cell counts provided are thus close to half of the actual total neuronal counts, except for TH-containing neurons of the PT projecting to both the striatum and the MLR, in which case all neurons from all sections were counted because of their rarity.

Semi-intact Preparation. To simultaneously record the activity of reticulospinal cells and locomotor movements, a semi-intact preparation was used. We used 13 larval animals for these experiments. The procedure was as described elsewhere (10, 35, 36). To expose the brain and the rostral segments of the spinal cord, skin, muscles, and surrounding tissues were removed from the rostral part of the animal, down to the caudal gills. The dorsal surface of the cranium was opened to obtain free access to the reticulospinal neurons in the MRRN. A transverse section was performed at the level of the habenula to eliminate the inputs from the basal ganglia and other rostral areas to the MLR. A dorsal midsagittal transection was per-

formed at the level of the diencephalon to provide access to the PT. The preparation was then transferred into the recording chamber. The cartilage containing the brain was pinned down to the bottom of a recording chamber covered with Sylgard (Dow Corning), whereas the intact body was left to swim freely in a video monitored adjacent chamber. The preparation was continually perfused with cold oxygenized Ringer solution (4 mL/min) and cooled to a temperature of 8 to 10 °C. A recovery time of at least 1 h after surgery was given before recording. When bath-applying DA onto the brain, the recording chamber was partitioned at the level of the caudal rhombencephalon with petroleum jelly, and the two partitions were independently perfused. Electrical stimulation of the PT (10-s train, 4–5 Hz, 4–30 μA, 2-ms pulses) elicited swimming movements during the experiments. At the end of the experiment, an electrolytic lesion (5 s, DC current, 10 μA) was performed to histologically control the location of the stimulation site (Fig. 3*D*).

Kinematic Recordings and Analysis. Locomotor movements of body were recorded (30 frames per second) by a video camera (HDR-XR200; Sony) positioned 1 m above the recording chamber. Locomotor movements were tracked and analyzed by using custom written scripts in Matlab (MathWorks) previously used in our laboratory (11, 35). Briefly, tracking markers were equidistantly distributed along the midline of the body by using geometrical analysis of the body. Swimming movements were monitored frame-by-frame through local measurement of the angle between the longitudinal axis of nonmoving parts of the body and the line drawn by two successive markers (35). The local curvature angles were determined throughout the whole body. This allowed us to observe that a mechanical wave was traveling rostrocaudally along the body, as expected during forward swimming. For further analysis, monitoring the body curvature of a single pair of markers at a specific point along the body (at 50% of body length) was sufficient to monitor the locomotor frequency, the number of locomotor cycles, and the duration of the locomotor bouts (35).

Isolated Brain Preparation. For experiments in an isolated brain preparation (10 larval animals for voltammetry experiments; 5 newly transformed and 1 larval animal for patch experiments), the same dissection procedure as described for the semi-intact preparation was performed, but the caudal body parts were removed after a complete transversal cut at the level of the first spinal cord segment.

Electrophysiological Recordings and Stimulation. Intracellular recordings of reticulospinal neurons in the MRRN region were performed as described elsewhere with the use of sharp microelectrodes (80–110 MΩ) filled with a 4 M potassium acetate solution (35–37). The signals were amplified by an Axoclamp 2A amplifier (sampling rate of 2–10 kHz; Axon Instruments) and acquired through a Digidata 1200 series interface coupled with Clampex 9.0 software (Axon Instruments) or AxoGraph X 1.4.4 (John Clements). Only reticulospinal neurons with a stable membrane potential, held for 5 min after impalement and lower than −60 mV, were included in the study. Extracellular recordings of reticulospinal neurons were performed by using a glass microelectrode filled with Ringer solution (tip diameter, 5 μm) and amplified with a microelectrode AC amplifier (bandwidth 100–500 Hz; model 1800; A-M Systems).

Homemade glass-coated tungsten microelectrodes (4–5 MΩ with 10-μm exposed tip) and a Grass S88 stimulator coupled to a Grass PSIU6 photoelectric isolation unit for controlling the stimulation intensity (Astro Med) were used for unilateral electrical stimulation of the PT. The stimulation site was chosen on the basis of previous anatomical and physiological studies (3, 10, 11). Electrical square pulses (2-ms duration) were applied with a frequency of 4 to 5 Hz for 10 s for train stimulation. A pause of 3 to 5 min was allowed between two train stimulations. Single stimuli at 0.1 Hz were used for eliciting excitatory postsynaptic currents. The stimulation intensities ranged from 4 to 35 μA. This would theoretically correspond to a maximum spread of the injected current ranging from 80 to 354 μm around the stimulation site (reviewed in ref. 38). In all types of preparations used in the present study, an electrolytic lesion was made at the end of the experiment to control histologically the location of the electrode (Fig. 3*D* shows semi-intact preparation; Fig. S2 *G–I* shows patch and voltammetry experiments in the isolated brain preparation).

Patch clamp was coupled with retrograde labeling to record targeted MLR neurons projecting to reticulospinal neurons on the basis of the protocol described elsewhere to record MLR cells projecting to respiratory networks (11). A surgery was made 24 h before the experiment. The animals were anesthetized with tricaine methanesulfonate (MS 222; 100 mg/L) and then transferred in a cold oxygenated Ringer solution (8–10 °C, 100% O_2). A 2-mm^2 flap window was opened on the top of the head to expose the caudal brainstem. MLR neurons were retrogradely labeled from an injection of Texas red–dextran amines [molecular weight (MW) of 3,000 Da; Molecular Probes] in the MRRN region. The incision was closed with Vetbond after the injection procedure. The animal was then returned to a nursery aquarium filled with oxygenated Ringer solution at room temperature. After maintaining the animal for 24 h to allow retrograde labeling of MLR cells, the brain was extracted and prepared for patch recordings. To access the MLR cells, the dorsal part of the isthmus and caudal mesencephalon was removed with a Vibratome in a cold Ringer solution (1–3 °C). The giant reticulospinal cell I1 was used as landmark to locate the MLR. Neurons were recorded under whole-cell patch clamp. Pipettes were pulled to a tip resistance of 4 to 6 MΩ. Bright-field and fluorescence imaging of the traced neurons were combined to allow targeted whole-cell patch recording of MLR cells projecting to the reticular formation. Patch pipette solution contained (in millimolar): cesium methane sulfonate 102.5, NaCl 1, $MgCl_2$ 1, EGTA 5, Hepes 5, ATP 0.3, GTP 0.1, and biocytin at 0.05%. Biocytin allowed us to identify the recorded cell. The pH was adjusted to 7.2 with CsOH, and the osmolarity to 240 mOsm with H_2O. Positive pressure was applied to the pipettes to allow tissue penetration by the electrode. Pressure was removed to allow a seal against the fluorescently labeled neurons. Recordings were made with a patch-clamp amplifier 2400 (A-M Systems).

Data analysis was performed by using ClampFit 10.0 (Axon Instruments), Spike2 5.19 (Cambridge Electronic Design), or Matlab 7.8 (MathWorks).

Voltammetry Recordings. DA concentration evoked by PT stimulation (10-s train, 5 Hz, 14–25 μA, 2-ms pulses) was locally measured by using fast-scan cyclic voltammetry with glass-insulated, Nafion-coated, carbon-fiber microelectrodes. As previously described (12), electrodes were made from individual carbon fibers (7-μm diameter; Goodfellow). Fibers were aspirated into glass pipettes (0.6 mm o.d., 0.4 mm i.d.; A-M Systems) and pulled on a vertical puller (Narishige). The glass seal was evaluated under light microscopy and the carbon fiber was cut to a length of 75 to 100 μm by using a scalpel. Following construction, the electrode was coated in Nafion (LQ-1105; Ion Power) and baked at 75 °C for 10 min. The electrodes were placed in the MLR and held at −0.4 V against Ag/AgCl between voltammetric scans and then driven to +1.3 V and back at 400 $V{\cdot}s^{-1}$ every 100 ms. Electroactive species within this voltage range oxidize and reduce at different points along the voltage scan and can be identified on the basis of their background-subtracted current by voltage (i.e., cyclic voltammogram) plots (12). Data were acquired and analyzed by using software written in LabVIEW 7.1 (National instruments). Stimulation artifacts were manually removed by interpolation. An electrolytic lesion (5 s, DC current, 10 μA) was performed in the recording site at the end of the experiment to verify histologically the location of the electrode (Fig. S2 *J* and *K*).

Drug Application. All drugs were purchased from Sigma and were diluted to their final concentration in Ringer solution. In some experiments, DA was bath-applied at a concentration of 10 μM. In other experiments, DA (5 mM) or the D1 receptor antagonist SCH 23390 (500 μM) were microinjected locally in the MLR, and D-glutamate (5 mM) was microinjected locally in the PT. As previously done in our laboratory (7, 8, 10, 11, 35, 37, 39), the microinjections were performed through a glass micropipette (tip diameter, 10–20 μm) by applying pressure pulses (3–4 psi) of various durations (20–100 ms) with a Picospritzer (General Valve) ipsilaterally to the stimulation and intracellular recording sites. Fast Green was added to the drug solution for visualizing the injection site as described elsewhere (e.g., refs. 10, 11, 37). The injected volumes were estimated by measuring the diameter of a droplet ejected in air from the tip of the pipette after applying a single pressure pulse. The volume of the droplet was calculated by using the equation of a sphere. The total volume of each microinjection was then estimated by multiplying this volume by the number of pulses used per microinjection, as previously done in our laboratory (e.g., refs. 7, 39). For each drug, the number of moles ejected was calculated. The size of the injections was also controlled visually under the microscope by measuring the spread of Fast Green at the level of the injection site in the brain tissue. The spread did not exceed 300 μm in diameter for any of these injections. This was also confirmed in four larval lampreys by measuring the spread of HRP [10% (wt/vol)] microinjection into the brain tissue (Fig. S2 *J* and *L*), as previously done by us (39). For bath applications and local drug injections, the drugs were washed out for a period of 1 h.

Statistics. Data in the text are presented as the mean ± SEM. The statistical analysis was performed by using Sigma Plot 11.0 (Systat) or Origin 7.0 (OriginLab). Statistical differences were assumed to be significant at $P < 0.05$. One-tailed paired Student *t* tests were used for comparing means between two groups. Correlations between variables were calculated using the Pearson product–moment correlation test.

ACKNOWLEDGMENTS. We thank Danielle Veilleux for technical assistance, Jean-François Gariépy for help with some of the experiments, and Frédéric Bernard for help with graphics. This work was supported by Canadian Institutes of Health Research Grants 15129 and 15176 (to R.D.), Parkinson Society Canada Grant 2011-11 (to R.D.), Fonds de la Recherche en Santé du Québec Groupe de Recherche sur le Système Nerveux Central (GRSNC) Grant 5249, Natural Sciences and Engineering Research Council of Canada Grant 217435 (to R.D.), National Institutes of Health Grant R01 MH 084874 (to S.A); Fonds de la Recherche en Santé du Québec fellowships (to D.R.); and a GRSNC Jasper Fellowship (to D.R.).

1. Kravitz AV, et al. (2010) Regulation of parkinsonian motor behaviours by optogenetic control of basal ganglia circuitry. *Nature* 466(7306):622–626.
2. Stephenson-Jones M, Samuelsson E, Ericsson J, Robertson B, Grillner S (2011) Evolutionary conservation of the basal ganglia as a common vertebrate mechanism for action selection. *Curr Biol* 21(13):1081–1091.
3. Pombal MA, El Manira A, Grillner S (1997) Afferents of the lamprey striatum with special reference to the dopaminergic system: A combined tracing and immunohistochemical study. *J Comp Neurol* 386(1):71–91.
4. Le Ray D, Juvin L, Ryczko D, Dubuc R (2011) Chapter 4—supraspinal control of locomotion: The mesencephalic locomotor region. *Prog Brain Res* 188:51–70.
5. Rolland AS, et al. (2009) Evidence for a dopaminergic innervation of the pedunculopontine nucleus in monkeys, and its drastic reduction after MPTP intoxication. *J Neurochem* 110(4): 1321–1329.
6. Beckstead RM, Domesick VB, Nauta WJ (1979) Efferent connections of the substantia nigra and ventral tegmental area in the rat. *Brain Res* 175(2):191–217.
7. Le Ray D, et al. (2003) Nicotinic activation of reticulospinal cells involved in the control of swimming in lampreys. *Eur J Neurosci* 17(1):137–148.
8. Smetana R, Juvin L, Dubuc R, Alford S (2010) A parallel cholinergic brainstem pathway for enhancing locomotor drive. *Nat Neurosci* 13(6):731–738.
9. Ménard A, Auclair F, Bourcier-Lucas C, Grillner S, Dubuc R (2007) Descending GABAergic projections to the mesencephalic locomotor region in the lamprey Petromyzon marinus. *J Comp Neurol* 501(2):260–273.
10. Derjean D, et al. (2010) A novel neural substrate for the transformation of olfactory inputs into motor output. *PLoS Biol* 8(12):e1000567.
11. Gariépy JF, et al. (2012) Specific neural substrate linking respiration to locomotion. *Proc Natl Acad Sci USA* 109(2):E84–E92.
12. Roitman MF, Wheeler RA, Wightman RM, Carelli RM (2008) Real-time chemical responses in the nucleus accumbens differentiate rewarding and aversive stimuli. *Nat Neurosci* 11(12):1376–1377.
13. Surmeier DJ, Ding J, Day M, Wang Z, Shen W (2007) D1 and D2 dopamine-receptor modulation of striatal glutamatergic signaling in striatal medium spiny neurons. *Trends Neurosci* 30(5):228–235.
14. Le Crom S, Kapsimali M, Barôme PO, Vernier P (2003) Dopamine receptors for every species: Gene duplications and functional diversification in Craniates. *J Struct Funct Genomics* 3(1-4):161–176.
15. Ericsson J, et al. (2013) Dopamine differentially modulates the excitability of striatal neurons of the direct and indirect pathways in lamprey. *J Neurosci* 33(18):8045–8054.
16. Blin M, Norton W, Bally-Cuif L, Vernier P (2008) NR4A2 controls the differentiation of selective dopaminergic nuclei in the zebrafish brain. *Mol Cell Neurosci* 39(4): 592–604.
17. Rink E, Wullimann MF (2001) The teleostean (zebrafish) dopaminergic system ascending to the subpallium (striatum) is located in the basal diencephalon (posterior tuberculum). *Brain Res* 889(1-2):316–330.
18. Marín O, Smeets WJ, González A (1997) Basal ganglia organization in amphibians: Catecholaminergic innervation of the striatum and the nucleus accumbens. *J Comp Neurol* 378(1):50–69.
19. Yamamoto K, Vernier P (2011) The evolution of dopamine systems in chordates. *Front Neuroanat* 5:21.
20. Puelles L, Verney C (1998) Early neuromeric distribution of tyrosine-hydroxylase-immunoreactive neurons in human embryos. *J Comp Neurol* 394(3):283–308.
21. Ericsson J, Silberberg G, Robertson B, Wikström MA, Grillner S (2011) Striatal cellular properties conserved from lampreys to mammals. *J Physiol* 589(pt 12):2979–2992.
22. Ericsson J, et al. (2013) Evolutionarily conserved differences in pallial and thalamic short-term synaptic plasticity in striatum. *J Physiol* 591(pt 4):859–874.
23. Pombal MA, El Manira A, Grillner S (1997) Organization of the lamprey striatum - transmitters and projections. *Brain Res* 766(1-2):249–254.
24. Robertson B, et al. (2012) The dopamine D2 receptor gene in lamprey, its expression in the striatum and cellular effects of D2 receptor activation. *PLoS ONE* 7(4):e35642.
25. Stephenson-Jones M, Ericsson J, Robertson B, Grillner S (2012) Evolution of the basal ganglia: Dual-output pathways conserved throughout vertebrate phylogeny. *J Comp Neurol* 520(13):2957–2973.
26. Grillner S, Robertson B, Stephenson-Jones M (2013) The evolutionary origin of the vertebrate basal ganglia and its role in action-selection. *J Physiol* 2013(Feb):25.
27. Schultz W, Dayan P, Montague PR (1997) A neural substrate of prediction and reward. *Science* 275(5306):1593–1599.
28. Thompson RH, Ménard A, Pombal M, Grillner S (2008) Forebrain dopamine depletion impairs motor behavior in lamprey. *Eur J Neurosci* 27(6):1452–1460.
29. Abalo XM, Villar-Cheda B, Anadón R, Rodicio MC (2005) Development of the dopamine-immunoreactive system in the central nervous system of the sea lamprey. *Brain Res Bull* 66(4-6):560–564.
30. Pierre J, Mahouche M, Suderevskaya EI, Repérant J, Ward R (1997) Immunocytochemical localization of dopamine and its synthetic enzymes in the central nervous system of the lamprey Lampetra fluviatilis. *J Comp Neurol* 380(1):119–135.
31. Pombal MA, Marín O, González A (2001) Distribution of choline acetyltransferase-immunoreactive structures in the lamprey brain. *J Comp Neurol* 431(1):105–126.
32. Quinlan KA, Buchanan JT (2008) Cellular and synaptic actions of acetylcholine in the lamprey spinal cord. *J Neurophysiol* 100(2):1020–1031.
33. Villar-Cerviño V, et al. (2006) Presence of glutamate, glycine, and gamma-aminobutyric acid in the retina of the larval sea lamprey: Comparative immunohistochemical study of classical neurotransmitters in larval and postmetamorphic retinas. *J Comp Neurol* 499(5): 810–827.
34. Barreiro-Iglesias A, Villar-Cerviño V, Villar-Cheda B, Anadón R, Rodicio MC (2008) Neurochemical characterization of sea lamprey taste buds and afferent gustatory fibers: Presence of serotonin, calretinin, and CGRP immunoreactivity in taste bud bi-ciliated cells of the earliest vertebrates. *J Comp Neurol* 511(4):438–453.
35. Brocard F, et al. (2010) The transformation of a unilateral locomotor command into a symmetrical bilateral activation in the brainstem. *J Neurosci* 30(2):523–533.
36. Sirota MG, Di Prisco GV, Dubuc R (2000) Stimulation of the mesencephalic locomotor region elicits controlled swimming in semi-intact lampreys. *Eur J Neurosci* 12(11): 4081–4092.
37. Brocard F, Dubuc R (2003) Differential contribution of reticulospinal cells to the control of locomotion induced by the mesencephalic locomotor region. *J Neurophysiol* 90(3): 1714–1727.
38. Ranck JB, Jr. (1975) Which elements are excited in electrical stimulation of mammalian central nervous system: a review. *Brain Res* 98(3):417–440.
39. Brocard F, Bardy C, Dubuc R (2005) Modulatory effect of substance P to the brain stem locomotor command in lampreys. *J Neurophysiol* 93(4):2127–2141.